MEDWIN PUBLISHERS
Committed to create value for Researchers

Physical Science & Biophysics Journal
ISSN: 2641-9165

First Principle Calculations of Phases Stability and Electronic Structure of the Trihalide Perovskite $RbSnBr_3$

Karima Benyahia[1]*, Bouchikhi S[2] and Bekhechi S[2]

[1]Faculty of Science, Belhadj Bouchaib University of Ain Temouchent, Ain Temouchent, Algeria

[2]Unity of Research "Materials and Renewable Energies", Faculty of Sciences, University of Abou-bekr Belkaid, 13000, Tlemcen, Algeria

Conceptual paper

Volume 3 Issue 3

Received Date: June 30, 2019

Published Date: August 05, 2019

***Corresponding author:** Karima Benyahia, Faculty of Science, Belhadj Bouchaib University of Ain Temouchent, Ain Temouchent, Algeria, Tel: 00213559359130; Email: benyahia_karima@yahoo.fr

Abstract

The most commonly used and studied halide perovskite is ABX_3, where A stands for Rb, B for Sn, and X for Br. A perovskite with high stability and ideal electronic band structure would be of essence, especially considering the materials used for solar cells. In this work, we have considered the two phases (cubic, orthorhombic) of $RbSnBr_3$. the two structures are studied to understand how are the crystal structure stability, band gap and the electronic properties including the total density of states and the projected densities of state have been studied, we found a good agreement with experiments and other calculations. The material has a band gap of 0.57 ev resulting from the transition Br 4P5 → Sn 5P2 that makes the material as a good perovskite compound candidate of a great interest for potential solar-cell applications.

Keywords: Halide perovskites; Phase stability; Electronic properties; Density functional theory (DFT)

Introduction

Perovskites are a large family of crystalline ceramics that takes their name from a specific mineral called (CaTiO3) because of their crystalline structure. As early as the 1990s, applications of perovskites underwent a major revolution thanks to their low cost for photovoltaic cells. Among the first tests is to introduce perovskite in a photovoltaic cell quadrupled to achieve yields of about 30%, exceeding the yield of silicon cells such as OLEDs (Organic Light Emitting Diodes), transistors and photo detectors [1,2]. Rubidium-tin III Bromine RbSnBr3 is a perovskite material considered among the class of luminescent materials, it has specific characteristics such that: the maximum emission wavelength is about 540 nm [3]. These characteristics are also used to use this material for applications based on the photo-luminous principle such as solar cells. Several studies have been made on luminescent materials [4-9], the two materials $RbSnCl_3$ and $RbSnI_3$ have been investigated in several studies [10].

Moreover, concerning the material $RbSnBr_3$, our research showed that no work was done except that it was the subject of a single experimental study based on the Raman spectrum measurement as a temperature function between 14 and 520 K [11]. Thanks to its low cost and its ease of transformation, the RbSnBr3 material

is used in several photovoltaic applications such as: solar cells based on DSSC (Dye-Sensitized Solar Cell) architecture [12], optoelectronic devices such as photodetectors [13], light-emitting diodes [14], lasers [15], thin-film transistors [16], and OILEDs [17]. $RbSnBr_3$ is characterized by a photoluminescence of high quantum efficiency, with a narrow spectral width, as well as its very low cost which makes it very attractive for industrialists. This prompts us to further explore this material which is characterized by such remarkable properties and applications in different fields. Our work aims to explore the structural and electronic properties of the three phases (cubic, orthorhombic and triclinic) of this material using the potential Pseudo formalism and the plane wave method "implemented in the Quantum Espresso code [18].

Methodology and Structure

The DFT calculations are performed in the QUANTUM ESPRESSO [14] simulation package with the PerdewBurke-Ernzerhof (PBE-GGA) [15] generalized gradient approximation (GGA) and plane-waves (PW) pseudopotentials. All calculations are performed with a cut-off of plane waves of 30 Ry and energy cut-off of 120 Ry. The Monkhorst k-point mesh used for these calculations is 6×6×6. The energy convergence of the calculated system is 1×10^{-6} eV.

The crystalline structure of RbSnBr3: Among the luminescent materials, there are the conductive materials which have the form, where A is an element of the group 1, such as: rubidium (Rb), B is the element from the group 14 such as tin (Sn), X is the element from the group 17 such as bromine (Br).

Structures

The space group of the cubic structure (Figure 1) of the material $RbSnBr_3$ is Pm^3. The orthorhombic structure (Figure 2), is characterized by the space group Pnmn. The triclinic structure (Figure 3), has a space group P1.

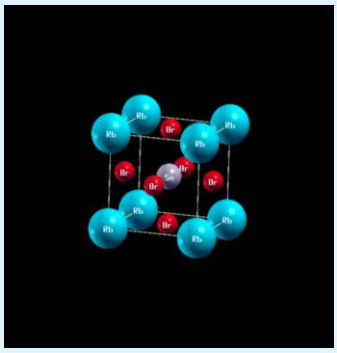

Figure 1: Cubic Structure of RbSnBr.

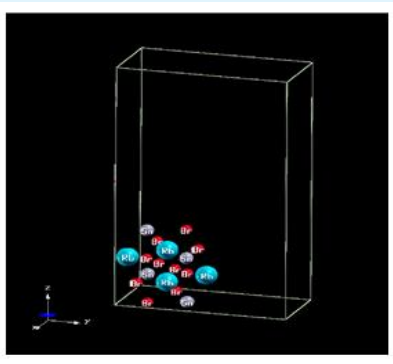

Figure 2: Orthorhombic Structure of $RbSnBr_3$.

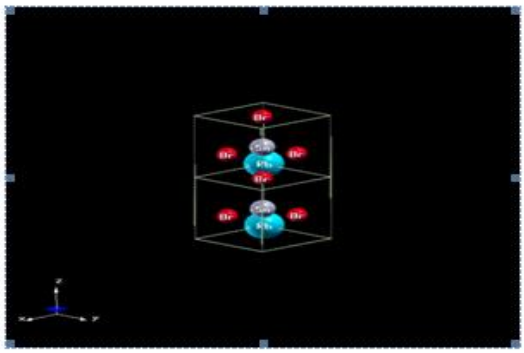

Figure 3: Triclinic Structure of $RbSnBr_3$.

Structural Properties

Determining the parameters of the equilibrium structure is the first and fundamental step. In this study, we explore the three phases: cubic, triclinic and orthorhombic of $RbSnBr_3$. The determination of the parameters of the equilibrium lattice, the bulk modulus of compressibility and its derivative are obtained by the extrapolation of the total energy versus the volume E_tot (eV) by the Murnaghan state equation [1]:

$$E(V) = \frac{BV}{B'}\left[\frac{(V_0/V)^{B'}}{B'-1} - 1\right] + cst \quad (1)$$

where $V_0, B\ et\ B'$ are respectively: the volume of the ground state, the compressibility modulus and its derivative.

The equilibrium volume is given by the minimum of the curve E_tot (V):

$$V = V_0\left(+\frac{B'P}{B_0}\right)^{-1/B'} \quad (2)$$

The compressibility modulus B is determined by the curvature of this curve:

$$B = V\frac{\partial^2 E}{\partial V^2} \quad (3)$$

And its derivative of the compressibility coefficient B 'is determined by fitage with the Murnaghan equation given by the following equation:

$$E(V) = E_0 + \frac{B_0}{B'(B'-1)}\left[V\left(\frac{V_0}{V}\right)^{B'} - V_0\right] + \frac{B_0}{B'}(V - V_0) \quad (4)$$

Figure 4 shows the curve of variation of total energy as a function of volume of $RbSnBr_3$ for the three phases, from which the equilibrium quantities (V0, a0, B0 and B ') can be obtained by the plane waves PW and the pseudopotential method and which are summarized respectively in the following (Tables 1-3):

Le matériau	Approximation	a (A^0) B(Gpa)	B' Total énergie
Cubic	PW, Pseudopotentiel	5.986 16.03	4.27 -1211.3475528
	Autre calcul	5.87	/

Table 1: The equilibrium parameter (A°), Total Energy (Ry) and the Bulk Modulus and its derivative (Gpa) for the cubic structure of $RbSnBr_3$.

Le matériau	Approximation	A (a.u) B(Gps)	B(a.u)	C(a.u)	B' Total Energie	Total
Orthorhombic	PW, Pseudopotentiel	8.83 150.78	18.01	33.91	1.002	-3700.86
	Autre calcul	8.6	18.55	31.31	/	/

Table 2: The equilibrium parameter (A°), Total Energy (Ry) and the Bulk Modulus and its derivative (Gpa) for the orthorhombic structure of $RbSnBr_3$.

Le matériau	Approximation	A(a.u) C(a.u)	B(a.u) B(Gpa)	B' Total Energie	Total
RbSnBr3	PW, Pseudopotentiel	11.61 37.13	11.04	12.07	5.3 -1213.83
	Autre calcul	11.083	11.088	11.094	/

Table 3: The equilibrium parameter (A°), Total Energy (Ry) and the Bulk Modulus and its derivative (Gpa) for the triclinic structure of $RbSnBr_3$.

The relaxed lattice parameters for the three phases of $RbSnBr_3$ are calculated and summarized in Table 1. they are compared with experimental data and other calculations to be a = 645.73(1) μm, b = 645.75(1) μm, c = 645.74(9) μm, which agree well with the experimental value of a = 627.6(4) μm [11]. For those compounds with a determined GGA band gap between 0.5—2.0 eV, we also perform beyond conventional DFT calculations using Heyd-ScuseriaErnzerhof (HSE) functional (i.e., HSE06) to get a more accurate determination of the band gaps [14-15]. The crystal structure of cubic MABX3 is shown in Fig. 1, where MA molecule takes the corner position, the metal element B takes the body center position, and the halide element X takes the face center position.

Band Gap, Total and Partial Density of State

To better understand the electronic properties of the cubic structure of RbSnBr3, it is also interesting and important to determine the total state densities in order to know what kind of hybridizations and which states are responsible in the bonding. To know the nature of the chemical bonds in this material, and the electronic transitions that can take place, we have calculated the total state density (TDOS) which reveals a semiconductor character for this material.

The calculated Total State Density (TDOS) is shown in Figure 4.

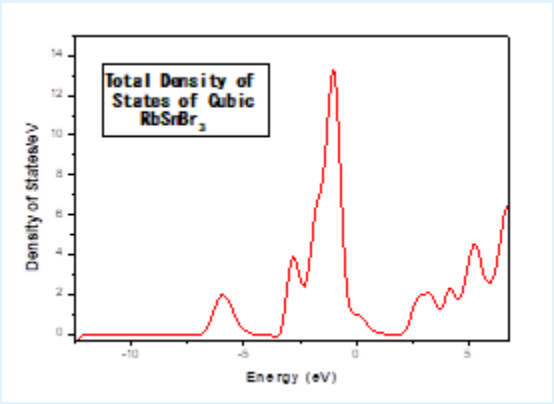

Figure 4: Total State Density (TDOS) of cubic structure of $RbSnBr_3$.

To better understand this total state density (TDOS), we calculated the partial state density of each element constituting the material $RbSnBr_3$.

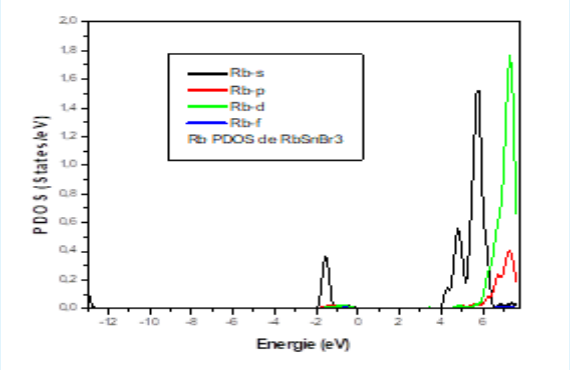

Figure 5: Partial Density of States of Rb.

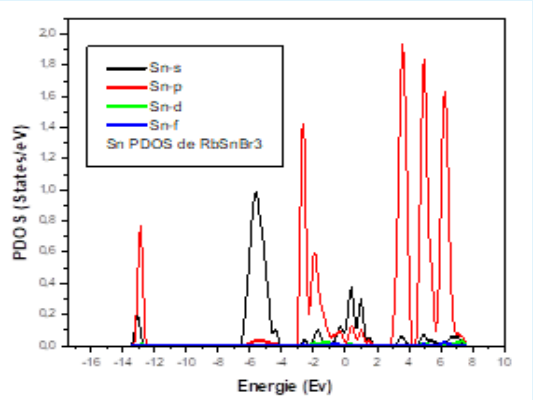

Figure 6: Partial Density of States of Sn.

For the Sn atom, we have a strong contribution of the p state in the conduction band and the valence band. For the states, the contribution in the valence band is average. The d State does not contribute in either the valence and the conduction bands.

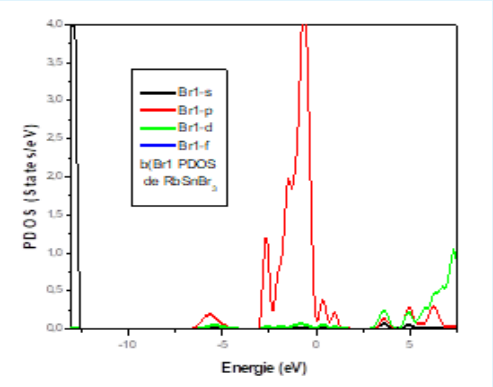

Figure 7: Partial Density of States of Br_1.

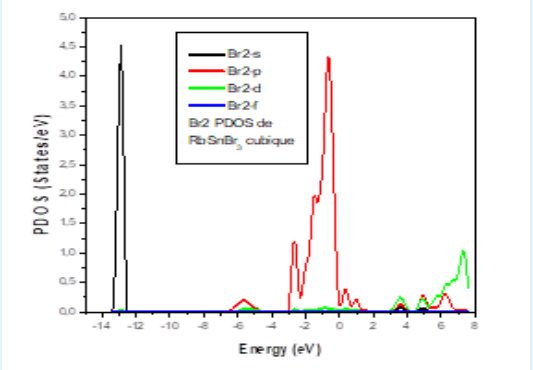

Figure 8: Partial Density of States of Br_2.

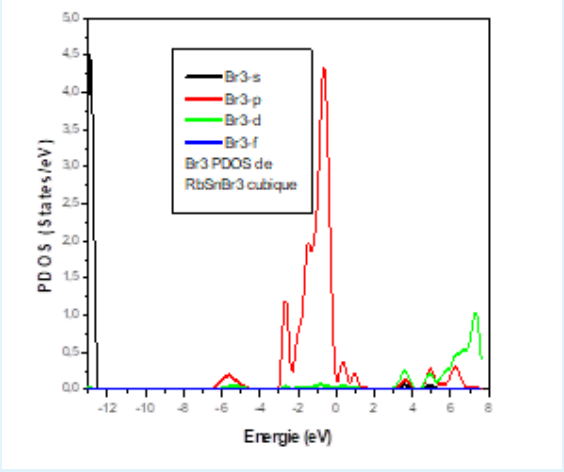

Figure 9: Partial Density of States Br_3.

It was found that the top of the valence bands mainly comprised 5p orbital of bromine, while the bottom of the conduction bands is dominated by the 4p orbital of tin.

Conclusion

The lattice parameters are in good agreement with those found experimentally and other calculations. The bulk modulus in the cubic and triclinic structures of $RbSnBr_3$ is weak, which shows that the material is not ductile, but we can see that its value is higher in the orthorhombic structure. The total energy reveals that the cubic phase is the most stable structure for $RbSnBr_3$. This material has not been investigated before and our calculations consist of a prediction. The total density of state of $RbSnBr_3$ reveals the semiconductor nature of this material. Moreover, the partial state densities of the different atomic species have shown that the valence band is characterized by a strong presence of the Br-P states, the Sn-P and Rb-s states, d, whereas the conduction band is dominated by the states Sn-P and Rb-s, d.

It was found that the top of the valence bands mainly comprised 5p orbital bromine, while the bottom of the conduction bands is dominated by the 4p orbit of tin. In this material, we found a transition from the electrons of the valence band to the conduction band Br $4P^5 \rightarrow$ Sn $5P^2$ corresponding to a small band gap of 0.57 eV which characterize this material as a good photonic absorber and yielded to identify $RbSnBr_3$ as a candidate perovskite compound of a great interest for potential solar-cell applications.

References

1. Im JH, Lee CR, Lee JW, Park SW, Park NG (2011) 6.5% Efficient Perovskite Quantum-Dot-Sensitized Solar Cell. Nanoscale 3(10): 4088-4093.

2. Kojima A, Teshima K, Miyasaka T, Shirai Y (2006) Novel Photoelectrochemical Cell with Mesoscopic Electrodes Sensitized by Lead-Halide Compounds (2). 210th ECS Meeting, Cancun, Mexico.

3. Dou L, Yang Y, You J, Hong Z, Chang WH (2014) Solution-Processed hybrid perovskite Phototectors with high detectivity. Nat Commun 5: 5404.

4. Tan ZK, Moghadam RS, Lai ML, Docampo P, Higler R, et al. (2014) Bright light-emitting diodes based on organometal halide perovskite. Nat Nanotechnol 9: 687-692.

5. Deschler F, Price M, Pathak S, Klinberg LE, Jarausch DD (2014) High photoluminescence efficiency and optically pumped lasing in solution-processed mixed halide perovskite semiconductors. J Phys Chem Lett 5(8): 1421-1426.

6. Chin XY, Cortecchia D, Yin J, Bruno A, Soci C (2015) Lead iodile perovskite light-emitting field-effect transistor. Nat Commun 6.

7. Era M, Morimoto S, Tsutsui T, Saito S (1994) Organic-inorganic heterostructure electroluminescent device using a layered perovskite semiconductor $(C_6H_5C_2H_4NH_3)_2PbI_4$. Appl Phys Lett 65(6): 676-678.

8. Chondroudis K, Mitzi DB (1999) Electroluminscence from an organic-inorganic perovskite incorporating a quarterhiophene dye within lead halide perovskite layers. Chem Mater 11(11): 3028-3030.

9. McCarty JG, Wise H (1990) Perovskite catalysts for methane combustion. Catal Today 8(2): 231-248.

10. Gldwasser MR, Rivas ME, Vockic EP (2014) Luminescent materials that emit light in the visible range or the near infrared range and methods of forming thereof. United States Patent.

11. Ketelaar JAA, Rietdijk FAA, Stavern CHV (1937) The crystal structure of ammonium, potassium, rubidium and cesium stannibromide. Rec Trav Chim 56(9): 907-908.

12. Kristin P (2016) Materials Data on $RbSnBr_3$ (SG:1) by Materials Project. 36 Materials Science.

13. Le site internet: Brillouni Zone.

14. Giannozzi P, Baroni S, Bonini N, Calandra M, Car R, et al. (2009) QUANTUM ESPRESSO: a modular and open-source software project for quantum simulations of materials. J Phys: Condens Matter 21(39).

15. Perdew JP, Burke K, Ernzerhof M (1996) Generalized Gradient Approximation Made Simple. Phys Rev Lett 77(18): 3865.

16. Monkhorst HJ, Parck DJ (1976) Special points for Brillouin-zone integrations. Phys Rev B 13(12): 5188-5192.

17. Birch F (1978) Finite strain isotherm and velocities for single-crystal and polycrystalline NaCl at high pressures and 300°K. J Geophys 83(B3): 1257-1268.

18. Krishnamoorthy T, Ding H, Yan C, Leong W, Baikie T, et al. (2015) Lead-free Germanium Iodide Perovskite Materials for Photovoltaic Application. J Mater Chem A 3(47): 23829-23832.